

Sporadic E layer development and disruption at low latitudes by prompt penetration electric fields during magnetic storms

M. A. Abdu,¹ J. R. Souza,¹ I. S. Batista,¹ B. G. Fejer,² and J. H. A. Sobral¹

Received 15 November 2012; revised 7 March 2013; accepted 8 April 2013; published 22 May 2013.

[1] An investigation of low-latitude sporadic E layers during magnetic storms shows that the formation and disruption of these layers are strongly controlled by the magnetospheric electric fields that penetrate to equatorial ionosphere. It is observed that a prompt penetration electric field (PPEF) of westward polarity that dominates the nightside ionosphere can cause formation of sporadic E layers near 100 km, while a PPEF of eastward polarity that dominates the dayside and eveningside can lead to disruption of an E_s layer in progress. It is shown that a vertical Hall electric field, induced by the primary zonal PPEF, in the presence of the storm-associated enhanced conductivity of the night E layer, can be responsible for vertical ion velocity convergence sufficient to influence the E_s layer formation. A downward polarity of the Hall electric field leads to E_s layer formation, while an upward polarity causes the E_s layer disruption. An interplay of magnetic storm associated prompt penetration electric field and energetic particle precipitation is evident in the observed E_s layer response features in the region of the South Atlantic/American magnetic anomaly reported here.

Citation: Abdu, M. A., J. R. Souza, I. S. Batista, B. G. Fejer, and J. H. A. Sobral (2013), Sporadic E layer development and disruption at low latitudes by prompt penetration electric fields during magnetic storms, *J. Geophys. Res. Space Physics*, 118, 2639–2647, doi:10.1002/jgra.50271.

1. Introduction

[2] Magnetospheric disturbances are well-known sources of ionospheric electric fields that can cause drastic modifications of the plasma distribution and dynamics of the equatorial and low-latitude ionosphere. Beginning with a storm development, magnetospheric electric fields promptly penetrate to equatorial and low-latitude ionosphere as an undershielding dawn-to-dusk electric field, which is soon followed by an overshielding electric field of opposite polarity and, after a delay of a few hours (3–4 h), by a disturbance wind dynamo electric field (DDEF), all of which produce large changes in the major phenomenology of the equatorial ionosphere. The equatorial ionization anomaly, the equatorial electrojet (EEJ), and the plasma bubble/equatorial spread F irregularity processes undergo drastic changes in the form of their enhanced occurrences or total suppressions depending upon the local time (LT) dependent actuation of these electric fields. Recent literatures based on observational and simulation studies have vastly improved our understanding of these electric fields and changes thereof that occur in the low-latitude ionosphere [Fejer, 2011; Fejer *et al.*, 2007; Abdu *et al.*, 2003b, 2007;

Kikuchi *et al.*, 1996; Huang *et al.*, 2005; Richmond *et al.*, 2003; Sobral *et al.*, 1997; Batista *et al.*, 1991; Greenspan *et al.*, 1991; Basu *et al.*, 2001; Spiro *et al.*, 1988]. Most of the published literatures on the storm time response of the low-latitude ionosphere have so far focused attention on the F region responses to disturbance electric fields and thermospheric winds. No study has so far been reported on the response of the low-latitude E region to the disturbance electric fields with the exception of a few papers on the EEJ responses which however are restricted to the dip equator only. In this paper, we present the response features of the low-latitude E region to storm time penetration electric fields, manifested as E_s layer response in the form of its anomalous development or disruption.

[3] In a typical event sequence, the interplanetary magnetic field (IMF) B_z turning south initiates a substorm marked by auroral electrojet (AE) activity intensification with rapid increase of high-latitude convection, when the convection electric field, undershielded by the region 2 current, promptly penetrates to equatorial latitudes as a dawn-dusk electric field. This prompt penetration electric field (PPEF), which is known as an undershielding electric field, has, in general, eastward (westward) polarity on the day (night) sector, and it presents peak intensity at the dusk (dawn) hours as a result of the ionospheric conductivity gradient that exists across the terminators. The enhanced convection also leads to the buildup of the shielding layer by the region 2 current, so that when the B_z turns northward marking a convection decrease, and/or an AE recovery, an overshielding electric field penetrates to equatorial latitudes which has a polarity local time dependence which is exactly opposite to that of the PPEF [e.g., Kelley *et al.*,

¹Instituto Nacional de Pesquisas Espaciais (INPE), Sao Jose dos Campos, Brazil.

²Center for Atmospheric and Space Sciences, Utah State University, Logan, Utah, USA.

Corresponding author: M. A. Abdu, Instituto Nacional de Pesquisas Espaciais (INPE), Sao Jose dos Campos, Brazil. (maabdu@dae.inpe.br)

1979; Fejer *et al.*, 2008]. The overshielding electric field is often followed by a disturbance wind dynamo electric field (DDEF) that sets in with a delay of 3–4 h from the storm initiation and has the same polarity local time dependence as that of the former [Blanc and Richmond, 1980; Fejer *et al.*, 2008; Richmond *et al.*, 2003]. In the results to be presented below, we will examine the responses of low-latitude sporadic E layers to disturbance electric fields under different storm phases and discuss the most likely electrodynamic processes that underlie such response features. Based on Digisonde observations at four equatorial and low-latitude sites in South America, we will demonstrate that a disturbance electric field, depending upon its polarity, can cause formation or disruption of sporadic E layers near 100 km. We will also propose a most likely mechanism that could explain these effects.

2. Generation of Sporadic E Layer at Low Latitudes During Intense Magnetic Storms

[4] Figure 1 shows the variations in the interplanetary and ionospheric parameters during the great storm of 29–30 October 2003. In the successive panels from top to bottom are shown the variations with UT of (1) the interplanetary magnetic field component B_z , (2) the auroral electrojet activity index AE , (3) the equatorial electrojet (EEJ) intensity represented by the geomagnetic field horizontal component ΔH over the dip equatorial site Jicamarca (after subtracting from it the corresponding ΔH of the off-equatorial site Piura), and (4) the F layer peak height $h_m F_2$ and the true heights at successive plasma frequencies from 3 MHz to the $f_o F_2$ over (a) Jicamarca (12°S , 76.9°W ; dip angle: 2°), (b) Sao Luis (2.33°S , 44.2°W ; dip angle: -3.85°), (c) Fortaleza (3.9°S , 38.45°W ; dip angle: -10.9°), and (d) Cachoeira Paulista (22.6°S , 315°E ; dip angle: -33.7°). The ΔH is obtained as the deviation of the H component at any time with respect to its value around a nearby quiet time midnight considered as a reference base. The superstorm of 29 October 2003 had its onset initiated by a shock event marked by the abrupt southward turning of the B_z at 0610 UT accompanied by storm sudden commencement and large AE intensification (up to ~ 5000 nT) indicated by arrow 1 [Zhao *et al.*, 2005; Lin *et al.*, 2005; Abdu *et al.*, 2007]. Very intense storm activity continued through a period that ended on 31 October. The data during the first 2 days when severe perturbations in the B_z and AE occurred are only plotted in this figure. The following important features of the storm onset and its impact on the equatorial ionosphere may be noted: (1) The B_z southward turning (with a large intensity of -38 nT) and the rapid AE intensification (with a large magnitude of ~ 4500 nT) occurred when it was past midnight over South American longitude (0110 LT for Peru and 0310 LT for Brazilian stations). (2) The sudden onset of a westward electrojet (counter electrojet, CEJ) at 0110 LT over JIC marked the presence of an equatorward propagating prompt penetration (undershielding) electric field (PPEF) of westward polarity. The CEJ rapidly attained large intensity (~ 150 nT) by 07 UT. (3) At the same time, an intense down drift of the F layer plasma caused a rapid descent of the layer (indicated by arrow 1) simultaneously over all the four stations JIC, SL, Fz, and CP. Over CP, the apparent lack of a clear layer descent is due to the layer upward movement caused by the prevailing thermospheric meridional wind [Abdu, 1997] (which is equatorward at night; see, for example, Emmert *et al.* [2002]) under the finite magnetic inclination (-34°). From model

calculations based on the Sheffield University plasmasphere-ionosphere model (SUPIM) [Bailey *et al.*, 1997], Batista *et al.* [2006] have estimated the descent velocity over SL to be around 130 m/s (3.5 mV/m). Over JIC, which is 2 h behind SL in local time, the corresponding descent velocity is expected to be smaller according to the LT dependence of the PPEF predicted from the magnetosphere-thermosphere-ionosphere electrodynamic general circulation model by Richmond *et al.* [2003] and from analysis of vertical drift data from ROCSAT-1 satellite observations by Fejer *et al.* [2008]. The apparently smaller descent rate of the F layer height over JIC as compared to that over SL in Figure 1 is in excellent agreement with these predictions. In the same LT zone as SL, the layer descent rate over Fz is smaller, which can be attributed to the effect of the layer uplift by the nighttime equatorward thermospheric wind (just as it was over CP) with the magnetic dip angles over Fz being around -11° . Descending to the heights of increasing recombination rate, the F layer eventually disappeared in the ionograms, and the disappearance lasted several minutes.

[5] Figure 2 shows the ionogram sequences during the period beginning with the F layer descent over all the four stations. (The ionograms were registered at a cadence varying from 10 to 15 min.) At SL, strong spread F activity was in progress at 0615 UT (0315 LT), the start of the storm. The spread F decreased in intensity with the rapid layer descent as can be clearly noted in the ionogram at 0715 UT (0415 LT). Additionally, we note the presence of a weak sporadic E layer (E_s layer) in the ionogram at 0615 UT with the top frequency, $f_i E_s$, of around 2.5 MHz that progressively increased to around 9 MHz in the ionogram taken at 0730 UT, marking a significant intensification of the E_s layer. Further, we note that the minimum frequency of the F layer trace in the ionogram at 0715 UT increased to 2.8 MHz from its value of ~ 1.5 MHz at 0645 UT, which represents a corresponding increase in the blanketing frequency of the E_s layer ($f_b E_s$). Since the parameter $f_b E_s$ is a measure of the plasma frequency of the E_s layer peak density, this result points to a significant increase, by a factor of ~ 4 , in the E_s layer peak density. We note further that the base height of the E_s layer that was slightly above 100 km in the first ionogram steadily decreased to less than 100 km in the last ionogram, which might be a direct consequence of a westward directed PPEF that prevailed during this period. The E_s layer trace also presented some degree of range spreading that increased with the trace evolution, at all the four stations. Similar behavior of the E_s layer evolution in terms of the intensity, the layer base height, and the echo range spreading can be identified in varying degrees in the ionograms at all the four sites, presented in Figure 2. Over Fortaleza, an E_s layer of moderate intensity was already in progress at the time of the storm onset. In the subsequent ionograms, the E_s activity intensified further as evidenced by the enhanced $f_i E_s$ of the trace, increased range spreading notable more at the lower frequencies, and additional oblique/higher-order traces at higher frequencies (as in the ionogram at 0650 UT) that transformed into intense range spreading increasing with frequency as at 0700 UT. The intensified E_s layer continued beyond 0720 UT. Over CP, the E_s layer was very weak before the storm onset. Following the storm onset, the layer intensified as evident from its multiple hop traces in the ionograms at 0630 and later, with the range spreading also intensified. Over JIC, the E_s layer

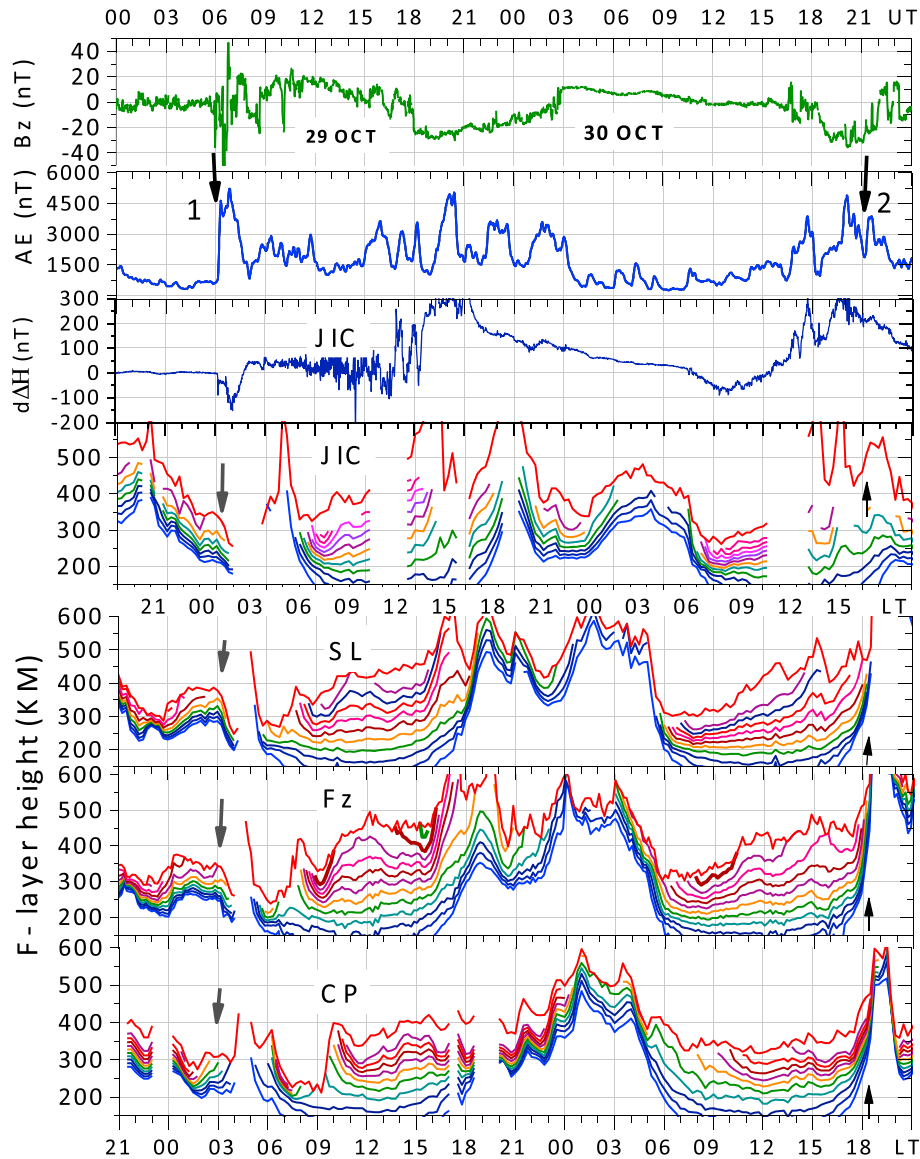


Figure 1. The upper three panels from top to bottom show the interplanetary magnetic field component B_z , the auroral electrojet (AE) activity index, and the equatorial electrojet intensity represented by $d\Delta H$ (JIC-PIU), the horizontal component of the geomagnetic field variation ΔH over Jicamarca (JIC) after subtracting from it the corresponding ΔH variation over the off-equatorial site Piura, in Peru, all at 1 min resolution. The lower four panels in descending order show the F layer peak height $h_m F_2$ (top curve in each panel) and the isolines of successive plasma frequencies at 1 MHz interval from 3 MHz to the $f_o F_2$, over Jicamarca (JIC), Sao Luis (SL), Fortaleza (Fz), and Cachoeira Paulista (CP) all at 10/15 min cadence.

was very weak at 06 UT (just before the storm onset) with an $f_i E_s \sim 2$ MHz. Under the influence of the strong westward PPEF, the layer soon increased in intensity as indicated by the large increase of $f_i E_s$ to >15 MHz in the ionogram at 07 UT. The layer appears to have started to disperse after 0715 UT. It is interesting to note that although there was enhanced range spreading of the E_s traces over JIC and SL as it was over all the four stations, there were no multiple hop traces over these stations, in contrast to their occurrence over CP and Fz. The possible implications will be discussed later. Another feature that may be noted is that the E_s layer base height over Fortaleza is somewhat lower than those over other stations in the beginning, while toward the end,

the base height over all the equatorial stations (SL, Fz, and JIC) was lower than that over the low-latitude site CP.

[6] Another case of a similar E region response, observed during the intense storm of 15 May 2005, is presented in Figure 3. In terms of the AE activity (maximum $AE \sim 2000$ nT), this storm is significantly less intense than the 29 October 2003 storm (with maximum $AE \sim 5000$ nT). We note in Figure 3a that the B_z turning south and the AE intensification starting at 0530 UT (0230 LT) produced a westward PPEF that first caused a slower F layer descent over Fz that soon accelerated, with the rapid AE intensification, at 0600 UT. At the lower heights attained by the F layer, the electron density soon decayed due to recombination.

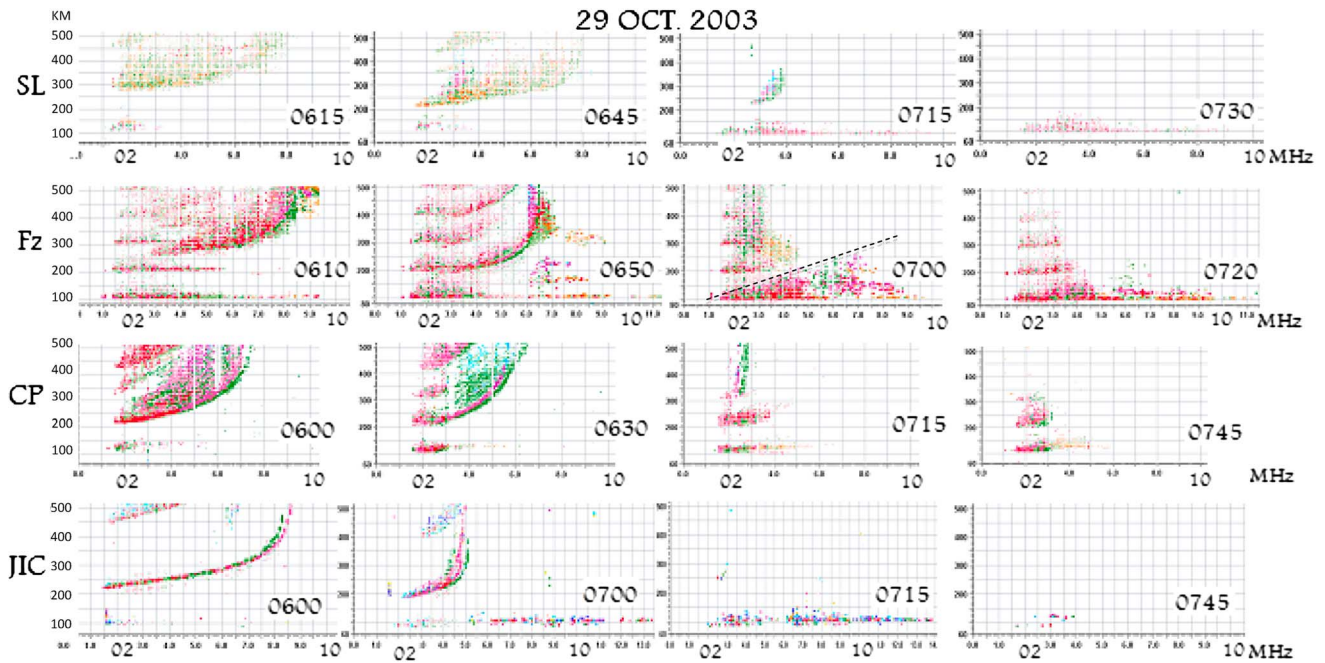


Figure 2. Ionograms starting at or before the 0610 UT storm onset on 29 October 2003, in rows, over Sao Luis (SL), Fortaleza (Fz), Cachoeira Paulista (CP), and Jicamarca (JIC). The slant dashed line in the Fz ionogram at 0700 UT is indicative of the similarity with the q-type E_s layer usually observed near the dip equator, believed to be produced by gradient drift instability process (see the text).

Intense spread F activity was in progress before the storm onset, and the rapid descent of the spread F trace starting at 0600 UT resulted in the decay of the irregularity structures (range spread F echoes) as can be noted in the ionogram at 0620 UT. In this ionogram, we also notice, as an important point, the formation of a night E layer with $f_oE = 2.2$ MHz. Its characterization as a typical E layer is justified by the group retardation of the virtual height clearly present at the f_oE . The formation of this layer may be considered as an evidence of nighttime ion production by energetic particle precipitation. We also note that range spreading echoes are present on the trace, suggesting some degree of irregularity structuring imbedded in the E layer. The E layer identity was, however, short lived as its evolution into an E_s layer is evident in the ionogram at 0640 UT. The PPEF was strongly westward during this period as can be verified from the rapid down drift of the F layer before its near disappearance due to recombination and/or blanketing by the E_s layer as seen in the ionogram at 0700 UT. The characteristics, such as the echo range spreading and the descending base height, are very similar to those observed in Figure 2. We note in this case that the E_s layer evolved from the night E layer in about 20 min, and its development continued till at least 0800 UT. The electrodynamics of the E_s layer formation process will be discussed in the next section.

3. Electrodynamics and Plasma Processes in Sporadic E Layer

[7] The results presented above clearly reveal the nature of the E layer response at dip equatorial and low latitudes in the South American longitude sector to PPEF occurring at night

hours when it has a westward polarity. Development of intense westward electrojet current (counter electrojet, CEJ) in response to strong westward PPEF at night hours has been reported before, during the 29–31 October storm sequence in the Asian longitude sector, by *Abdu et al.* [2007]. Here we are reporting such nighttime CEJ in the American longitude sector. However, we will not discuss this aspect in detail except to point out that this result should serve as an evidence for the presence of enhanced E layer conductivity at night produced by a storm-related ionization source as was shown also in the paper by *Abdu et al.* [2007]. Our main focus in this paper is on the low-latitude E_s layer response to the PPEF identified as such for the first time. In explaining these results, we need to consider the fact that the basic process of vertical ion convergence that operates in the E_s layer formation should result in (1) a thin layer of enhanced density responsible for the f_bE_s and/or multiple hop traces and (2) development of large-scale vertical gradients (with respect to the layer peak) that should lead to irregularity growth by instability process, responsible for the range spreading echoes and the f_iE_s .

[8] As regards the aspect 1 above, it has been known that over low latitudes, normally under quiet conditions, and in the height region near 100 km (as in the cases studied here), the vertical convergence of ionization for the formation of a thin layer can occur mainly by field line perpendicular transport caused by a zonal wind with/without a vertical shear in it [*Abdu et al.*, 2003b]. In the present case however, we need to identify a mechanism not based on winds but instead on the PPEF found to be responsible for these E_s layers. In other words, we need to examine the ability of a PPEF to bringing about a vertical ionization convergence and density redistribution thereof that could lead to the formation of a thin layer

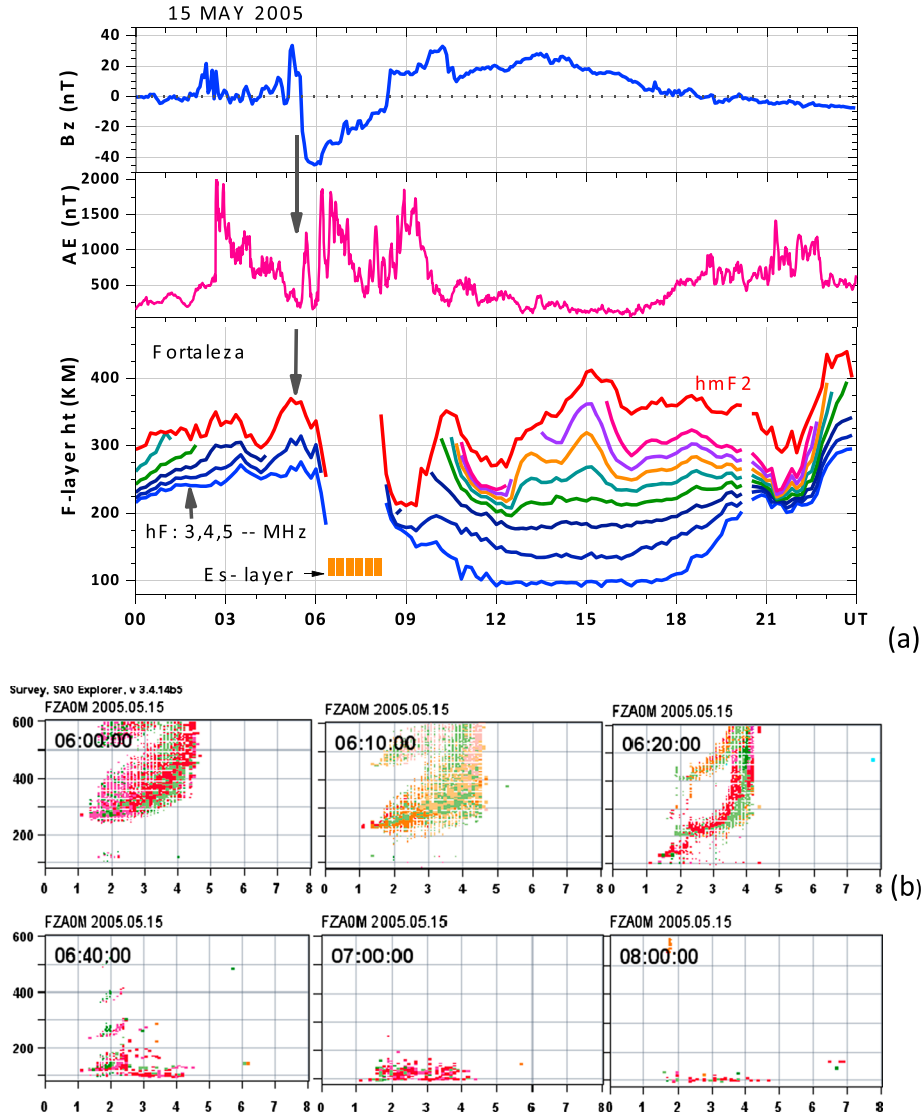


Figure 3. (a) One minute values of (top panel) the IMF B_z and (middle panel) the AE indices during the 15 May 2005 storm and (bottom panel) the $h_m F_2$ and isolines of successive plasma frequencies from 3 MHz to the $f_o F_2$ over Fz. The B_z turning south with AE intensification causes a slow F layer descent at 0530 UT soon to become a rapid descent with a second and more intense AE increase at 0600 UT. E or E_s layer formation is indicated by a horizontal bar starting at \sim 0620 UT. (b) Sequential ionograms over Fortaleza from 0600 UT to 0800 UT showing the evolution of the spread F and E_s layer traces following the storm onset. Note the formation of a night E layer in the 0620 UT ionogram that preceded the E_s layer formation.

that can present the observed E_s layer characteristics. It is known, as has been shown also by *Abdu et al.* [2003b], that at the height region of our interest where $v_{in}/\omega_I > 1$ (where v_{in} is the ion-neutral collision frequency and ω_I the ion gyrofrequency), the vertical transport of ionization is more efficient by a vertical electric field (E_z) than by a zonal electric field (E_y), as can be verified from the equation [*Abdu et al.*, 2003b] for vertical ion velocity (v_z) given by

$$v_z = \frac{R_i}{1 + R_i^2} \left[\frac{E_z}{B_0} - \frac{E_y}{B_0 R_i} - U_y \right] \quad (1)$$

[9] Here, $R_i = v_{in}/\omega_I > 1$ (for the E_s layer height 120 km), U_y is the zonal wind which we ignore here, and

B_0 is the magnetic field. Thus, considering only the vertical electric field, the vertical ion convergence thereof can be shown as given by [*Abdu et al.*, 2003b]

$$\frac{dv_z}{dz} = \frac{1}{R_i} \left[-\frac{E_z}{B_0 H_n} + \frac{dE_z}{dz B_0} \right] \quad (2)$$

[10] Here H_n is the neutral atmosphere scale height. Equation (2) shows that the vertical convergence in v_z can be produced by a “steady” E_z as indicated by the first term and/or by its height gradient as represented by the second term. The source of this electric field can be attributed to Hall conduction, driven by the primary PPEF, which is a zonal electric field (westward in this case), in the presence of an enhanced E layer conductivity

according to the simplified relationship: $E_z = (\Sigma_H/\Sigma_P)E_y$, $\Sigma_{H,P}$ being the field line integrated Hall or Pedersen conductivities (for a more general relationship between E_z and E_y , see *Haerendel et al.* [1992]) [*Abdu et al.*, 1998, 2003b, 2003a]. The Hall electric field will be established meridionally across the magnetic field lines in the height region of the enhanced Hall mobility peaking near 120 km. Its intensity is dependent inversely on the field line integrated Pedersen conductivity (Σ_P) arising from higher levels along any given magnetic field line. Clear indication of enhanced nighttime ion production that can cause E layer conductivity enhancement is evident from (1) the formation of a night E layer over Fortaleza with $f_oE \cong 2.3$ MHz as seen in the ionogram at 0620 UT, in Figure 3, and (2) the intense counter electrojet over Jicamarca during 0610–0800 UT, with peak $\Delta H_{(JC-PJU)} \cong -150$ nT as seen in Figure 1. The source of the enhanced ionization is believed to be storm-enhanced energetic particle precipitation. In the SAMA (South Atlantic magnetic anomaly) region in which the present observations were made, there is also other independent and indirect evidence for storm-enhanced E region ionization/conductivity attributed to energetic particle precipitation [see, for example, *Abdu et al.*, 2005; *Batista and Abdu*, 1977].

[11] In a simple approach, we may first make an estimate of the E_z that can lead to a dv_z/dz sufficient enough to produce an E_s layer with the observed characteristics in terms of the ratio of its peak to ambient density. For an approximate estimate, we may consider the $f_oE \sim 2.5$ MHz ($N = 6.6 \times 10^{10}/\text{m}^3$) of the night E layer observed in Figure 3 to be representative of a typical case of the background density produced by the storm time ionization source. Based on the degree of blanketing, the top frequency of the second hop trace of the E_s layer may be taken to represent the f_bE_s which thus is found to be ~ 3.5 MHz (that is, $N_{\text{max}} = 1.5 \times 10^{11} \text{ m}^{-3}$) as per the ionograms at 0700 and 0720 UT over Fz in Figure 2. These values yield a ratio N_{max}/N_0 of the order of 2.5. On the basis of the continuity equation for E_s layering, which includes contributions from vertical ion convergence and diffusion terms, and assuming quasi-steady conditions, we can arrive at a value of $dv_z/dz \approx 3 \text{ m s}^{-1} \text{ km}^{-1}$ as that is required to produce an N_{max}/N_0 of 2.5 [see *Abdu and Batista*, 1977, Figure 5a]. Equation (2) can be used to estimate the value of E_z required to produce this value of $dv_z/dz \approx 3 \text{ m s}^{-1} \text{ km}^{-1}$, that is compatible with the observed N_{max}/N_0 ratio. The contribution of the second term of equation (2) to the ion convergence can be assumed to be small as compared to that of the first term (as can be verified from the generally slow gradient in the Σ_H/Σ_P distribution with the apex height to be shown in Figure 4). Thus, using values of R_i and H_n appropriate for 100 km, we obtain $E_z \approx -12$ mV/m, which we may consider as the *minimum value* of the vertical electric field required to produce the observed E_s layer density ratio.

[12] We can now verify if the value of the E_z obtained above is compatible with that which can be induced by the PPEF (E_y) as per the relationship: $E_z = (\Sigma_H/\Sigma_P)E_y$. For this, we performed a calculation of Σ_H/Σ_P under night hours covering the local time interval of the observed effect. The field line integrated conductivities were calculated using the ion density altitude-latitude distribution (extending from the dip equator to $\pm 20^\circ$ magnetic latitude) as obtained from the Sheffield University plasmasphere-ionosphere model (SUPIM) [*Bailey et al.*, 1997] simulation runs. Here we used a SUPIM version that was modified to extend the lower height limit of calculation from its

original 120 km to 90 km. To simulate the storm-enhanced night E region ion density, the ion production rate that is normally calculated from the scattered solar UV radiation input in the model is now complemented by an additional ion production rate due to energetic particle precipitation (IPEP) that could lead to an $f_oE \approx 2.5$ MHz of the night E layer observed over Fortaleza (in Figure 3) and that increased (arbitrarily) to 4 MHz near the latitude of CP closer to the central region of the SAMA. The IPEP rate was calculated for a precipitating electron flux in the energy range of 8–28 keV, using an electron energy spectral shape extrapolated from that reported by *Mann et al.* [1963]. An electron density profile thus obtained is shown in Figure 4a for 0400 LT (for -2.3° latitude). The field line integrated conductivities were calculated as a function of the equatorial apex altitudes up to 800 km. Figures 4b and 4c show the local time variation of the conductivity ratio as a function of the apex altitude, without and with the enhanced ionization, respectively. We note that enhancement in Σ_H/Σ_P , associated with the additional ionization, in Figure 4c as compared to the quiet time values in Figure 4b, is evident in a considerable extent of the apex height or equivalently in magnetic latitude range $\pm 19^\circ$. Here we need to point out that while Σ_H arises mostly from E layer heights (around 120 km), Σ_P arises from higher up altitudes and in the F region all along a given field line between conjugate E layers, which is strongly dependent on the thermospheric meridional winds as well. We made adjustments in the HWM93 (Horizontal Wind Model 1993) winds [*Hedin et al.*, 1996] so that the prestorm nighttime F layer plasma density distribution as well as the poststorm F layer density depletion due to strong westward PPEF is reasonably well accounted for. Thus, we may note that E layer density enhancement due to energetic particle precipitation and the thermospheric winds both contribute to the apex height dependent local time variation of the ratio Σ_H/Σ_P in the model simulation result presented in Figure 4. In Figure 4, Σ_H/Σ_P presents significant enhancement following the enhanced E region ion production rate introduced at the start of the storm. At any specific local time in the course of the enhanced ion production rate, the value of the conductivity ratio varies also with the apex height. Increase up to four in this ratio may be noted at larger apex height (higher latitudes) and up to nine at lower apex height, that is, closer to the equator. It needs to be pointed out that the latitude/apex height variation of the conductivity ratio should depend also on how precisely the horizontal winds used in the SUPIM could reproduce the prestorm F region ion distribution along the field line coupled to the E region where storm time enhanced conductivity should be taking place.

[13] We may now examine if the minimum value of the vertical Hall electric field (determined above as $E_z \approx -12$ mV/m), required to produce the observed density enhancements of the E_s layers (in the cases studied here), can be induced by the primary zonal PPEF (E_y) based on their relationship $E_z = (\Sigma_H/\Sigma_P)E_y$. As pointed out before (section 2), the value of the E_y during the peak of the event in Figure 1 was around 3.5 mV/m which therefore yields a ratio $\Sigma_H/\Sigma_P \sim 3.4$. This value of the field line integrated conductivity ratio may be considered to be the minimum required for the E_s layer formation with the observed density ratio of N_{max}/N_0 , and it is found to be well within the range of values simulated for this ratio in Figure 4. Thus, we are in a position to conclude that the observed major E_s layer feature (the density enhancement ratio) is consistent with the

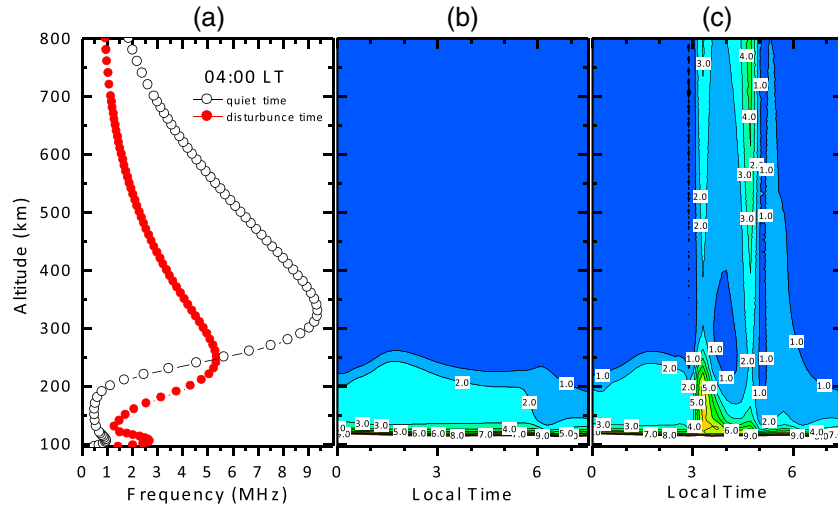


Figure 4. (a) Electron density-height profiles calculated by the SUPIM comparing a quiet time equatorial (2.3°) reference profile at 04 LT with the profile calculated (under a strong westward penetration electric field) immediately after the storm onset including the storm-enhanced E region density peak (red curve). The local time variation starting at midnight in (b) the field line integrated conductivity ratio (Σ_H/Σ_P) calculated for a quiet day plotted as a function of the magnetic field line apex altitude and (c) the field line integrated conductivity ratio calculated for the electron density profiles resulting from the PPEF and extra E region ionization effect that started at 0310 LT.

layer formation arising from a Hall vertical electric field induced by the primary PPEF of westward polarity.

[14] As a further test of validity of the proposed mechanism, we examined the possibility if a PPEF of eastward polarity could produce an opposite effect on the E_s layer development, that is, if an E_s layer already in progress can be disrupted by an eastward electric field (that is, an upward vertical Hall electric field). Figure 5 presents a sequence of ionograms showing an interesting case of E_s layer disruption later during the continuing activity of the same storm sequence (29–30 October 2003) that is plotted in Figure 1. On the evening of 30 October, a large uplift of the F layer occurred over SL, Fz, and CP. As reported by *Abdu et al.* [2008], this was the result of an intense PPEF of eastward polarity that occurred, with an AE intensification (by ~ 2000 nT), under the B_z south condition that prevailed at this time, indicated by arrow number 2 in Figure 1. As can be noted in Figure 5, an E_s layer activity was already in progress at 21 UT (18 LT) over Fortaleza. With the uplift of the layer that started at this time, the E_s became weaker and a further layer rise caused the total disruption of the E_s layer. It may be recalled that postsunset E_s layer disruption associated with the F layer height rise under the quiet time prereversal enhancement in zonal electric field/vertical drift was demonstrated by *Abdu et al.* [2003a]. In that case, the E_s layer disruption was explained as caused by a vertical electric field [see also *Carrasco et al.*, 2007] that was part of the plasma vortex flow of the evening equatorial ionosphere [*Kudeki and Bhattacharyya*, 1999].

[15] The second aspect of the vertical ion convergence for E_s layer formation concerns the development of plasma irregularities that produced the range spreading E_s layer traces over all the four sites. The layer density enhancement causing radio wave reflection and hence multiple hop traces was present only over Fz and CP, however. They were absent over JIC and SL that are closer to the dip equator where

the vertical velocity convergence for layer formation and the resulting layer peak density enhancement appear to operate less efficiently than at locations farther away from the dip equator. But, density gradients sufficient to cause growth of irregularities responsible for the range spreading E_s layer traces did develop over all these sites. In all the cases, the range spreading echoes must originate from coherent backscattering at HF from decameter size irregularities formed by the gradient drift instability mechanism. The instability grows when the density gradient is parallel to an imposed electric field [see, for example, *Fejer and Kelley*, 1980]. In the present case, the E_z is directed downward, and therefore, we expect the irregularities to be generated at topside of the E_s layers. This point can be verified from the precise structure of the range spread traces. Although they do not present similar characteristics at the different sites, there are some cases that provide the necessary indications to this effect. For example, in the ionogram at 0700 UT over Fortaleza (in Figure 2), we have drawn a slant dashed line marking what looks like an upper boundary of the range spread of the E_s layer increasing with the frequency of the ionogram. The pattern appears like that of an equatorial q-type E_s layer trace. As the probing frequency increases, the radio waves penetrate the layer bottomside to access the irregularity sampling height region at increasing oblique angles, thus explaining the systematic increase of spreading range with frequency. This shows that the irregularities are indeed generated at the negative gradient region of the E_s layer topside under the presence of the downward Hall electric field.

[16] As a complementary information, we need to point out that the generation of the Hall electric field by the primary zonal electric field will be significant enough only to the extent that the extra ionization occurs preferentially in the height region of Hall mobility (near 120 km). We may make a comment here that an increase of ionization at

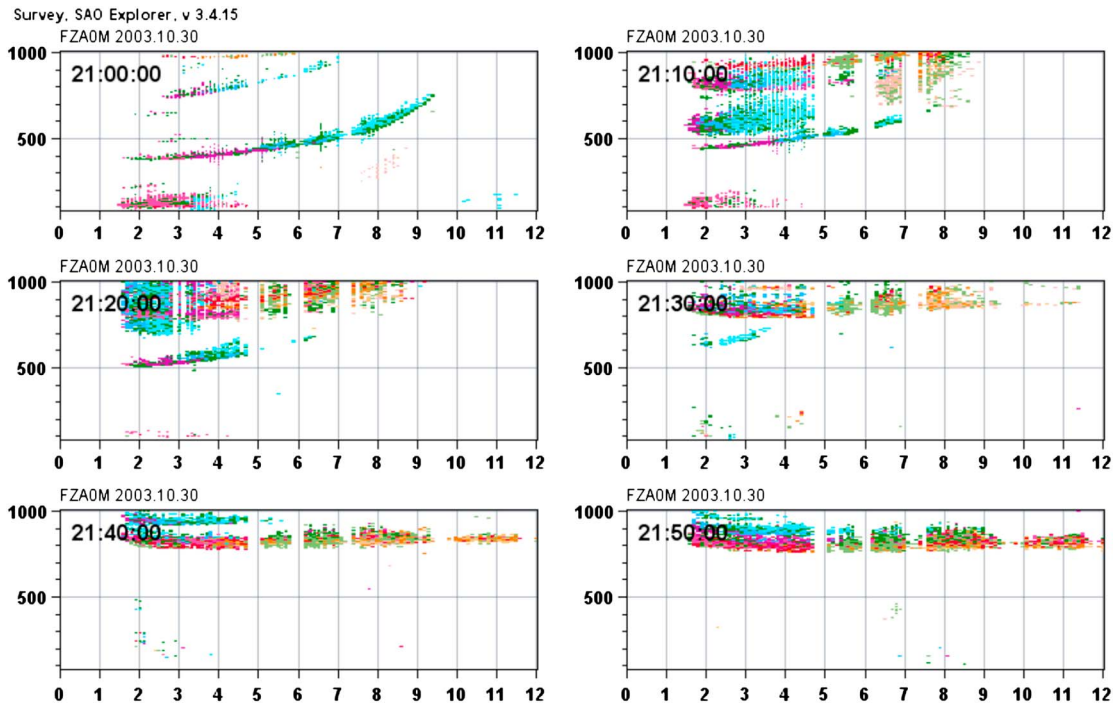


Figure 5. Ionograms over Fortaleza showing E_s layer disruption in association with a rapid uplift of the F layer under a strong PPEF of eastward polarity in the evening hours (starting at 21 UT in this case) during the 30 October 2003 superstorm.

any height will cause proportional increases in the local values of the Hall and Pedersen conductivities, thereby not necessarily modifying the ratio of local values of these conductivities. The situation is different, however, when we consider the magnetic field line integrated value of the conductivity ratio, Σ_H/Σ_P , which controls the development of the vertical/meridional Hall electric field, E_z . A preferential increase of ionization in the E region, of enhanced Hall mobility, is required for producing an increase in the ratio Σ_H/Σ_P . An extra ionization in a wider height region covering also that of the large Pedersen mobility (near 140 km and in the F region) may not produce an increase in the Σ_H/Σ_P ratio required for the vertical electric field development. But, this situation is very unlikely to occur because the energy distribution of the precipitating particles should suffer modification as the azimuthally drifting inner radiation belt particles reach their longitude of precipitation, in this case, the SAMA region. While the longitudinal drift rate (or gradient drift rate) is primarily dependent on the energy of the particles, it is also influenced by the magnetospheric electric field [Ziauddin and Abdu, 1978], which, in this case, is the prompt penetration electric field at low latitudes (the PPEF). The degree of the electric field influence/control is dependent on the energy of the precipitating electrons in the spectral range that affect the height region of our interest (near and above 100 km). The electric field influence increases with the decrease in energy (that is, decrease in drift rate) of the precipitating electrons. In this way, the electron precipitation dominating the height region of Hall conductance will be displaced in longitude with respect to that of the Pedersen conductance, since the energy of the precipitating electrons in the former case (10–15 keV) is significantly higher than that in the latter case (2–3 keV).

4. Conclusions

[17] The results presented here though based only on a few case studies provide evidence for the effect of storm time prompt penetration electric fields on the electron density distribution and structuring of the low-latitude E region. We have observed more cases of such manifestations of the PPEF effects (not presented here) that serve to confirm the consistency of these results. The main conclusions of the present study can be stated as follows.

[18] 1. Storm time magnetospheric electric fields penetrating to equatorial latitudes can cause significant modifications to the electron density distribution and structuring of the E layer near 100 km. A westward PPEF during night hours is found to cause formation of sporadic E layers, while an eastward electric field such as is present in the evening sector can cause the disruption of an E_s layer in progress. 1. Vertical electric field arising from Hall conduction induced by the primary zonal electric field (PPEF) is capable of causing the vertical ion drift and its vertical gradient, leading to the ionization convergence needed to produce the observed sporadic E layer characteristics.

[19] 2. Although not evaluated quantitatively, the downward gradient region of the E_s layer topside, in the presence of the parallel/downward vertical electric field, leads to instability development and irregularity formation, which seems to be responsible for the range spreading traces associated with the E_s layer.

[20] So far, similar results have not been reported for other longitudes, which might suggest that these effects are likely peculiar to the longitude sector of the South Atlantic/South American magnetic anomaly (SAMA) region, where it has been known that storm-associated ionospheric conductivity enhancements do occur as we have demonstrated also through

the present results. In any case, it will be worth investigating if similar PPEF effects could be operating at other longitude sectors as well. In this context, it may be recalled that predawn E layer conductivity enhancement indicated by a westward equatorial electrojet has been observed over the Pacific equatorial site, Yap, during intense magnetic storms [Abdu et al., 2007; Fejer et al., 2007].

[21] **Acknowledgments.** This work was supported by the Conselho Nacional de Desenvolvimento Científico e Tecnológico (CNPq) through the process CNPq 300883/2008-0. The IMF data were obtained from the ACE satellite site <http://www.srl.caltech.edu/ACE/>. The Jicamarca Radio Observatory is a facility of the Instituto Geofísico del Perú operated with support from NSF AGS-0905448 through Cornell University. The Jicamarca Digisonde data were downloaded from the site <http://umlcar.uml.edu/DIDBase>.

[22] Robert Lysak thanks the reviewers for their assistance in evaluating this paper.

References

- Abdu, M. A. (1997), Major phenomena of the equatorial ionosphere-thermosphere system under disturbed conditions, *J. Atmos. Sol. Terr. Phys.*, *59*, 1505–1519.
- Abdu, M. A., and I. S. Batista (1977), Sporadic E-layer phenomena in the Brazilian geomagnetic anomaly: Evidence for a regular particle ionization source, *J. Atmos. Terr. Phys.*, *39*, 723–731.
- Abdu, M. A., P. T. Jayachandran, J. MacDougall, J. F. Cecile, and J. H. A. Sobral (1998), Equatorial F region zonal plasma irregularity drifts under magnetospheric disturbances, *Geophys. Res. Lett.*, *25*, 4137–4140.
- Abdu, M. A., J. MacDougall, I. S. Batista, J. H. A. Sobral, and P. T. Jayachandran (2003a), Equatorial evening prereversal electric field enhancement and sporadic E layer disruption: A manifestation of E and F region coupling, *J. Geophys. Res.*, *108*(A6), 1254, doi:10.1029/2002JA009285.
- Abdu, M. A., I. S. Batista, H. Takahashi, J. MacDougall, J. H. Sobral, A. F. Medeiros, and N. B. Trivedi (2003b), Magnetospheric disturbance induced equatorial plasma bubble development and dynamics: A case study in Brazilian sector, *J. Geophys. Res.*, *108*(A12), 1449, doi:10.1029/2002JA009721.
- Abdu, M. A., I. S. Batista, A. J. Carrasco, and C. G. M. Brum (2005), South Atlantic magnetic anomaly ionization: A review and a new focus on electrodynamic effects in the equatorial ionosphere, *J. Atmos. Sol. Terr. Phys.*, *67*, 1643–1657.
- Abdu, M. A., T. Maruyama, I. S. Batista, S. Saito, and M. Nakamura (2007), Ionospheric responses to the October 2003 superstorm: Longitude/local time effects over equatorial low and middle latitudes, *J. Geophys. Res.*, *112*, A10306, doi:10.1029/2006JA012228.
- Abdu, M. A., et al. (2008), Abnormal evening vertical plasma drift and effects on ESF and EIA over Brazil-South Atlantic sector during the 30 October 2003 superstorm, *J. Geophys. Res.*, *113*, A07313, doi:10.1029/2007JA012844.
- Bailey, G. J., N. Balan, and Y. Z. Su (1997), The Sheffield University ionosphere-plasmasphere model—A review, *J. Atmos. Terr. Phys.*, *59*(13), 1541–1552.
- Basu, S., S. Basu, K. M. Groves, H.-C. Yeh, S.-Y. Su, F. J. Rich, P. J. Sultan, and M. J. Keskinen (2001), Response of the equatorial ionosphere in the South Atlantic region to the great magnetic storm of July 15, 2000, *Geophys. Res. Lett.*, *28*, 3577–3580.
- Batista, I. S., and M. A. Abdu (1977), Magnetic storm associated delayed sporadic-E enhancements in the Brazilian geomagnetic anomaly, *J. Geophys. Res.*, *82*, 4777–4783.
- Batista, I. S., E. R. de Paula, M. A. Abdu, N. B. Trivedi, and M. E. Greenspan (1991), Ionospheric effects of the March 13, 1989, magnetic storm at low and equatorial latitudes, *J. Geophys. Res.*, *96*, 13,943–13,952.
- Batista, I. S., M. A. Abdu, J. R. Souza, F. Bertoni, M. T. Matsuoka, P. O. Camargo, and G. J. Bailey (2006), Unusual early morning development of the equatorial anomaly in the Brazilian sector during the Halloween magnetic storm, *J. Geophys. Res.*, *111*, A05307, doi:10.1029/2005JA011428.
- Blanc, M., and A. D. Richmond (1980), The ionospheric disturbance dynamo, *J. Geophys. Res.*, *85*, 1669–1686.
- Carrasco, A. J., I. S. Batista, and M. A. Abdu (2007), Simulation of the sporadic E layer response to prereversal associated evening vertical electric field enhancement near dip equator, *J. Geophys. Res.*, *112*, A06324, doi:10.1029/2006JA012143.
- Emmert, J. T., B. G. Fejer, G. G. Shepherd, and B. H. Solheim (2002), Altitude dependence of middle and low-latitude daytime thermospheric disturbance winds measured by WINDII, *J. Geophys. Res.*, *107*(A12), 1483, doi:10.1029/2002JA009646.
- Fejer, B. G. (2011), Low latitude ionospheric electrodynamics, *Space Sci. Rev.*, *158*, 145–166, doi:10.1007/s11214-010-9690-7.
- Fejer, B. G., and M. C. Kelley (1980), Ionospheric irregularities, *Rev. Geophys.*, *18*, 401–454.
- Fejer, B. G., J. W. Jensen, T. Kikuchi, M. A. Abdu, and J. L. Chau (2007), Equatorial ionospheric electric fields during the November 2004 magnetic storm, *J. Geophys. Res.*, *112*, A10304, doi:10.1029/2007JA012376.
- Fejer, B. G., J. W. Jensen, and S.-Y. Su (2008), Seasonal and longitudinal dependence of equatorial disturbance vertical plasma drifts, *Geophys. Res. Lett.*, *35*, L20106, doi:10.1029/2008GL035584.
- Greenspan, M. E., C. E. Rasmussen, W. J. Burke, and M. A. Abdu (1991), Equatorial density depletions observed at 840 km during the great magnetic storm of March 1989, *J. Geophys. Res.*, *96*, 13,931–13,942.
- Haerendel, G., J. V. Eccles, and S. Cakir (1992), Theory of modeling the equatorial evening ionosphere and the origin of the shear in the horizontal plasma flow, *J. Geophys. Res.*, *97*, 1209–1223.
- Hedin, A. E., et al. (1996), Empirical wind model for the upper, middle and lower atmosphere, *J. Atmos. Terr. Phys.*, *56*, 1421–1447.
- Huang, C.-S., J. C. Foster, and M. C. Kelley (2005), Long-duration penetration of the interplanetary electric field to the low-latitude ionosphere during the main phase of magnetic storms, *J. Geophys. Res.*, *110*, A11309, doi:10.1029/2005JA011202.
- Kelley, M. C., B. G. Fejer, and C. A. Gonzales (1979), An explanation for anomalous ionospheric electric fields associated with a northward turning of the interplanetary magnetic field, *Geophys. Res. Lett.*, *6*, 301–304.
- Kikuchi, T., H. Luhr, T. Kitamura, O. Saka, and K. Schlegel (1996), Direct penetration of the polar electric field to the equator during a DP2 event as detected by the auroral and equatorial magnetometer chains and the EIS-CAT radar, *J. Geophys. Res.*, *101*, 17,161–17,173.
- Kudeki, E., and S. Bhattacharyya (1999), Postsunset vortex in equatorial F region plasma drifts and implications for bottomside spread F, *J. Geophys. Res.*, *104*, 28,163–28,170.
- Lin, C. H., A. D. Richmond, J. Y. Liu, H. C. Yeh, L. J. Paxton, G. Lu, H. F. Tsai, and S.-Y. Su (2005), Large-scale variations of the low-latitude ionosphere during the October–November 2003 superstorm: Observational results, *J. Geophys. Res.*, *110*, A09S28, doi:10.1029/2004JA010900.
- Mann, G. L., S. D. Bloom, and H. I. Jr. West (1963), The electron spectrum from 90 to 1200 keV as observed on Discoverer satellites 29 and 31, in *Space Research III*, edited by W. Priestner, pp. 447–462, North Holland Publishing Co, Amsterdam, The Netherlands.
- Richmond, A. D., C. Peymirat, and R. G. Roble (2003), Long-lasting disturbances in the equatorial ionospheric electric field simulated with a coupled magnetosphere-ionosphere-thermosphere model, *J. Geophys. Res.*, *108*(A3), 1118, doi:10.1029/2002JA009758.
- Sobral, J. H. A., M. A. Abdu, W. D. Gonzalez, B. T. Tsurutani, I. S. Batista, and A. L. C. Gonzalez (1997), Effects of intense storms and substorms on the equatorial ionosphere/thermosphere system in the American sector from ground-based and satellite data, *J. Geophys. Res.*, *102*, 14,305–14,314.
- Spiro, R. W., R. A. Wolf, and B. G. Fejer (1988), Penetration of high latitude electric field effects to low latitudes during SUNDIAL 1984, *Ann. Geophys.*, *6*, 39–50.
- Zhao, B., W. Wan, and L. Liu (2005), Response of equatorial anomaly to the October–November 2003 superstorm, *Ann. Geophys.*, *23*, 693–706.
- Ziauddin, S., and M. A. Abdu (1978), On the apparent equatorward propagation of auroral substorm absorption events at low auroral latitudes, *Can. J. Phys.*, *56*, 1412–1417.